Supplementary Information

**Efficient and stable perovskite mini-module *via* high quality homogeneous perovskite crystallization and improved interconnect**

Haitao Zhou[1,2], Kai Cai[1,2], Shiqi Yu[1,2], Zhenhan Wang[1,2], Zhuang Xiong[1,2], Zema Chu[1,2], Xinbo Chu[1,2], Qi Jiang[1,2] & Jingbi You[1,2]*

[1]Laboratory of Semiconductor Physics, Institute of Semiconductors, Chinese Academy of Sciences, P. R. China, 100083.

[2]Center of Materials Science and Optoelectronics Engineering, University of Chinese Academy of Sciences, Beijing, P. R. China, 100049.

*Corresponding author: jyou@semi.ac.cn

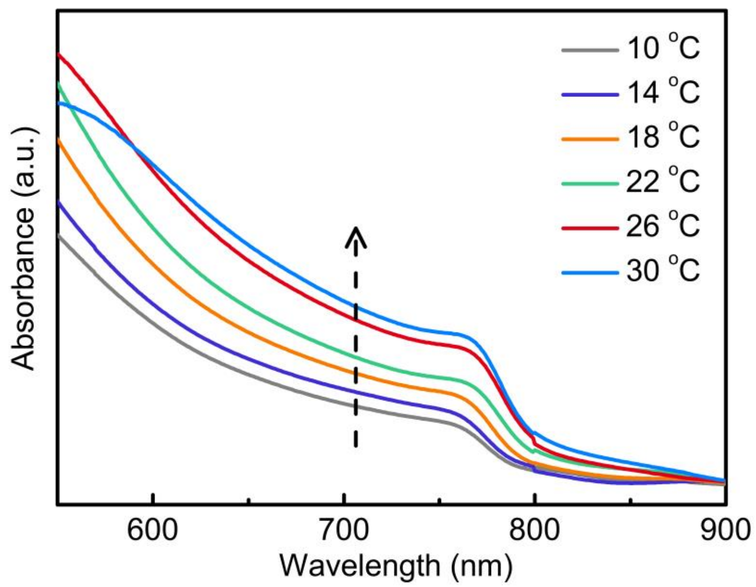


**Supplementary Fig. 1 |** Absorption of intermediate films grown at different LTSG temperatures.

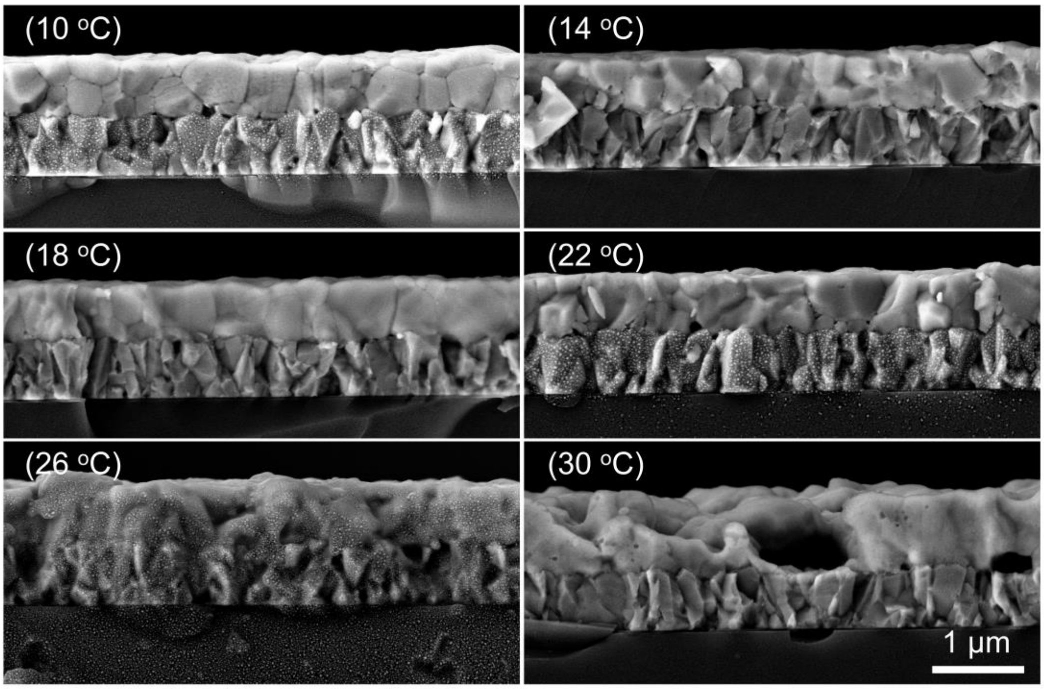


**Supplementary Fig. 2 |** Cross-sectional SEM morphologies of perovskite films fabricated at different LTSG temperatures.

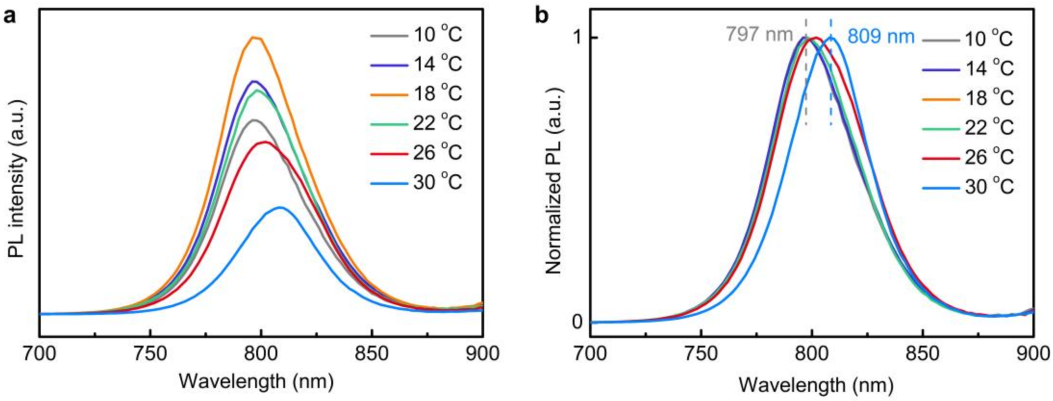


**Supplementary Fig. 3 |** Steady-state PL spectrum of a perovskite films (a) and its normalized representation (b).

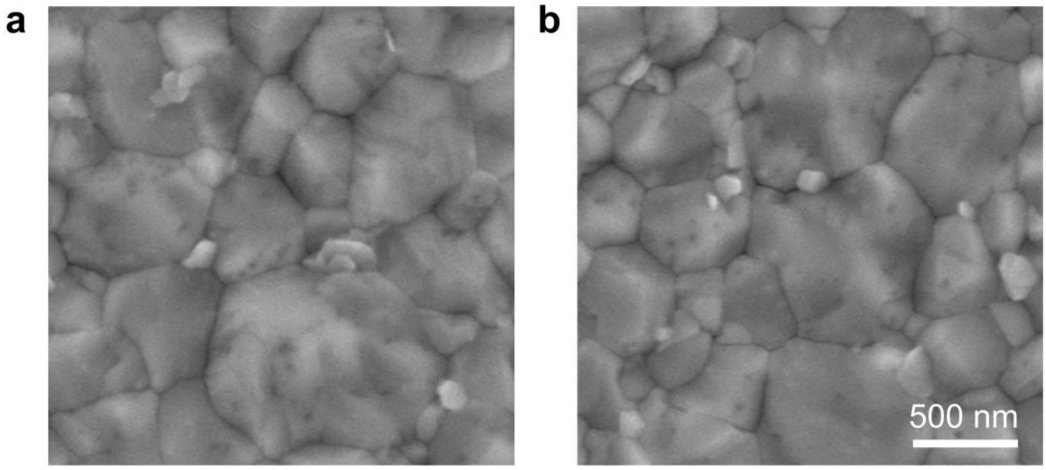


**Supplementary Fig. 4 |** Surface SEM morphology of perovskite films fabricated at 26 $^{o}$C (**a**) and 35 $^{o}$C (**b**) ambient temperature, while the LTSG temperatures were both 18 $^{o}$C.

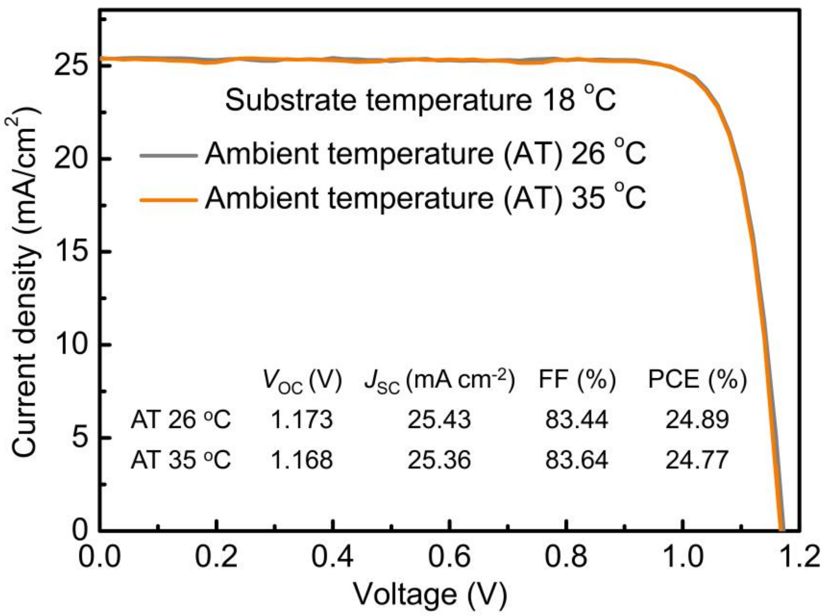


**Supplementary Fig. 5 |** *J-V* curves and performance parameters of devices constructed with perovskite films prepared at ambient temperatures of 26 °C and 35 °C respectively.

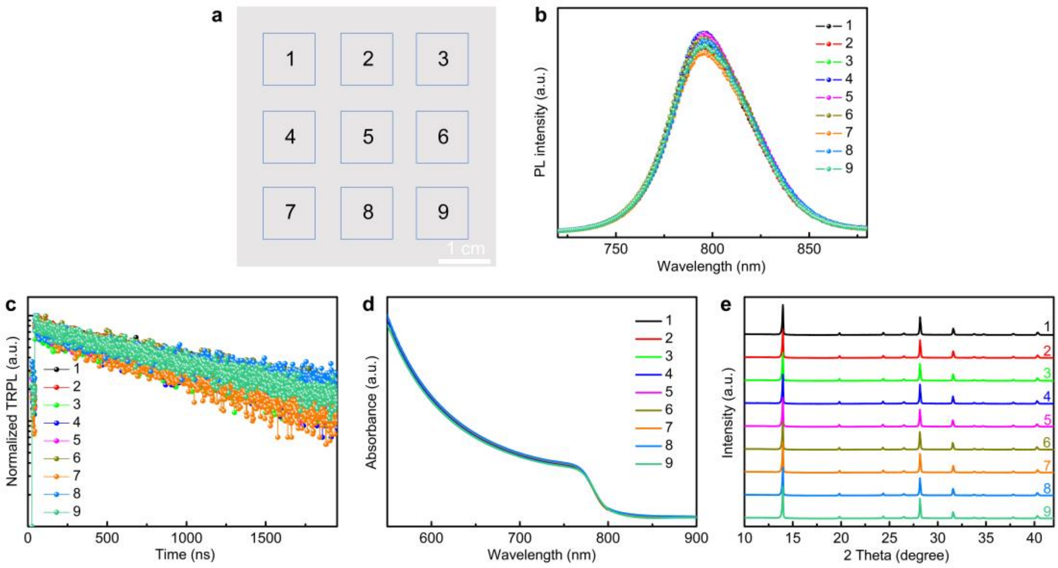


**Supplementary Fig. 6 | a,** Schematic illustration of the fabricated large-area perovskite film cut into 9 pieces. **b**, Photoluminescence spectra, **c,** TRPL patterns, **d,** Absorption spectra and **e,** XRD patterns of 9 areas of a 5 cm × 5 cm LTSG based perovskite films.

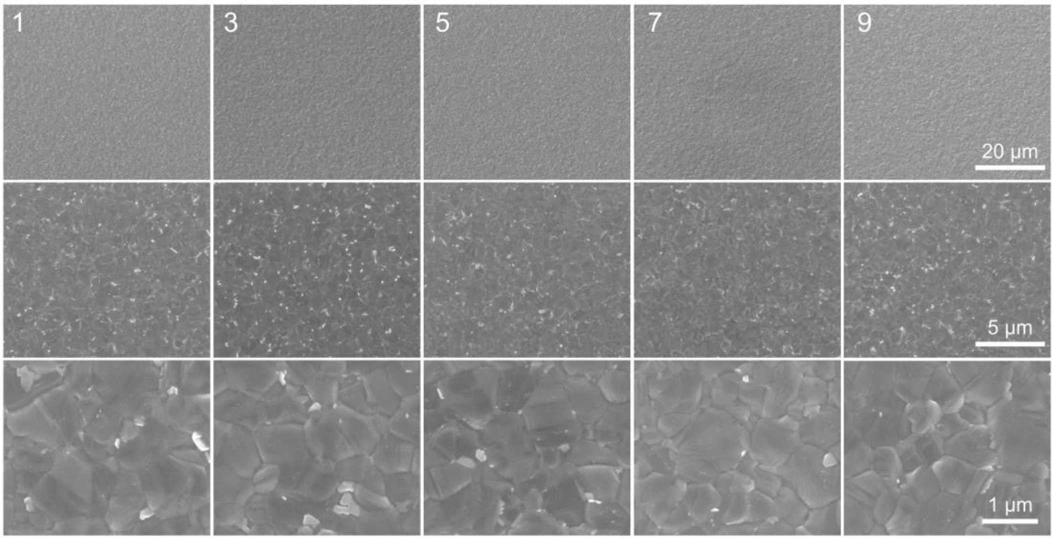


**Supplementary Fig. 7 |** Surface SEM images of different areas of the large-area films at different magnifications in Supplementary Fig. 6a. Uniform and similar shapes can be seen.

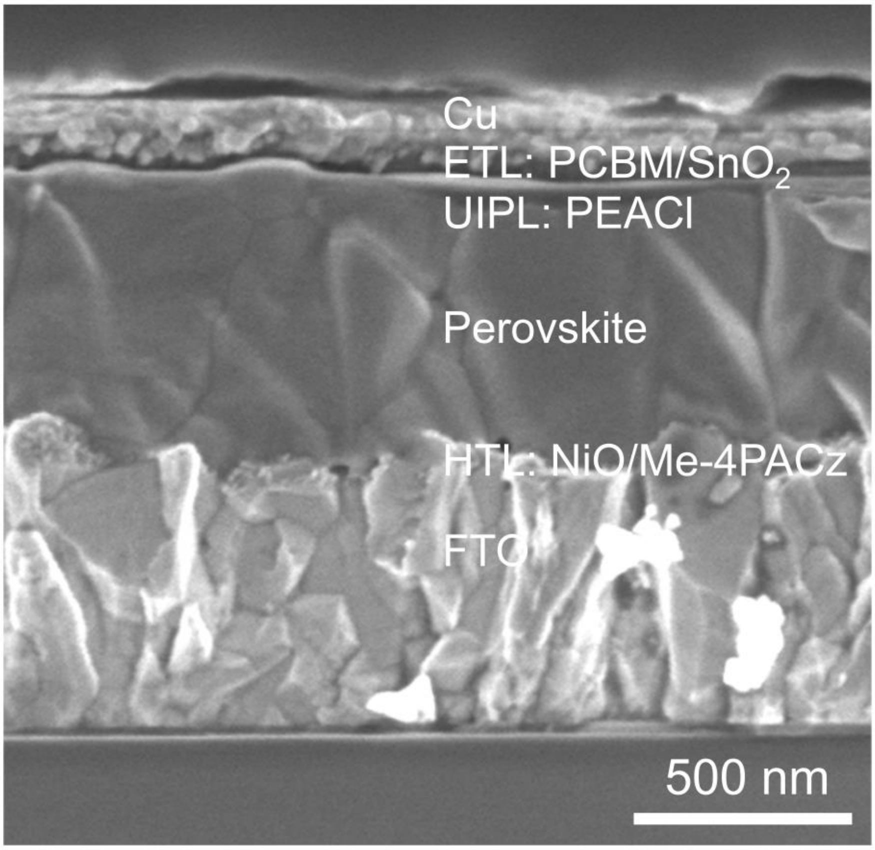


**Supplementary Fig. 8 |** Cross-sectional SEM image of our inverted perovskite solar cell.

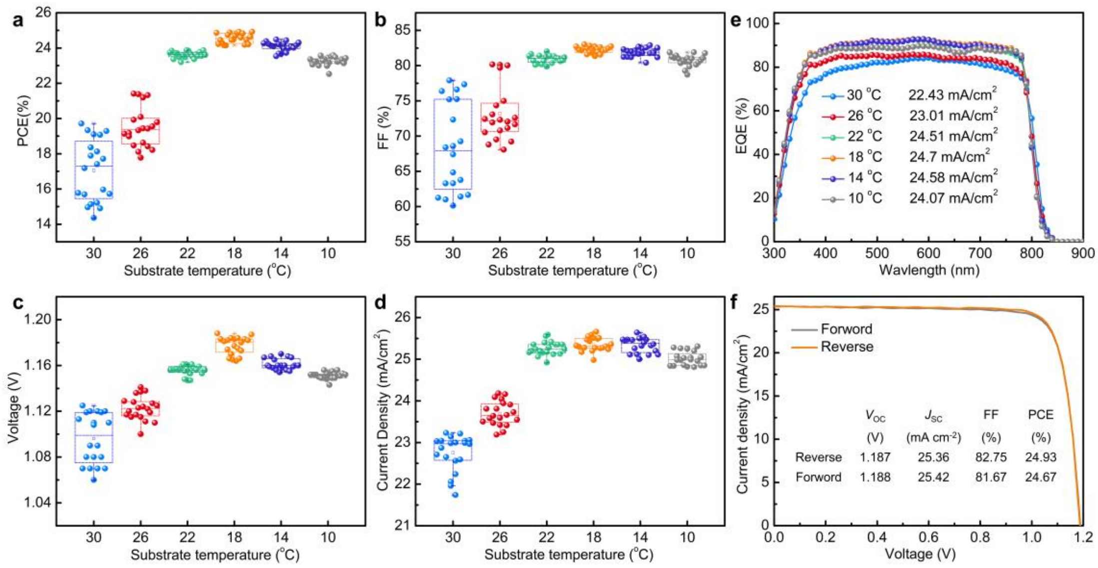


**Supplementary Fig. 9 |** Statistical distribution of (**a**) PCE, (**b**) FF, (**c**) $V_{OC}$ and (**d**) $J_{SC}$ obtained from *J-V* curves of small-area (aperture area 0.0737 $cm^2$) cells with different LTSG temperatures. **e,** EQE spectrum and integrated short circuit current density of the devices. **f,** LTSG-18 °C optimizes the forward and reverse *J-V* curves and performance parameters of the device.

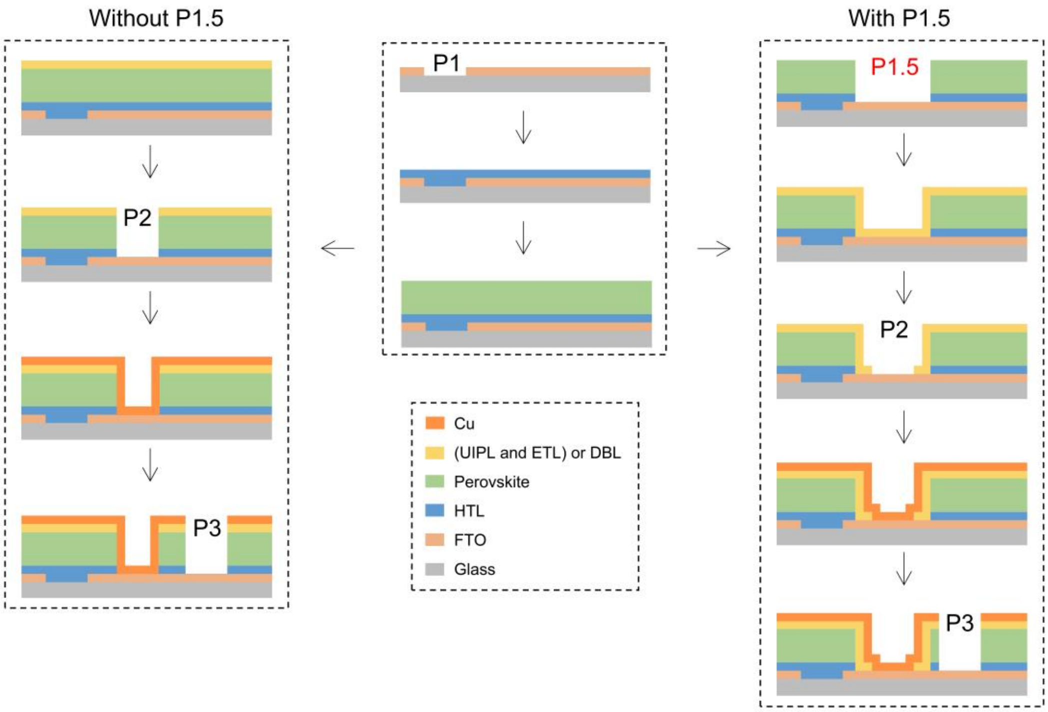


**Supplementary Fig. 10 |** Manufacturing process of the perovskite solar modules with and without P1.5 (DBL).

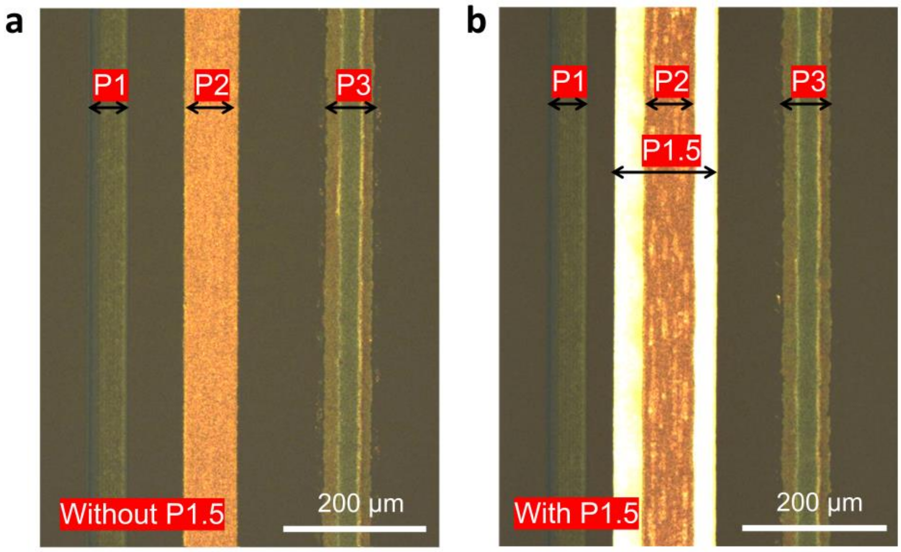


**Supplementary Fig. 11 |** Optical microscope images of interconnected regions with and without P1.5.

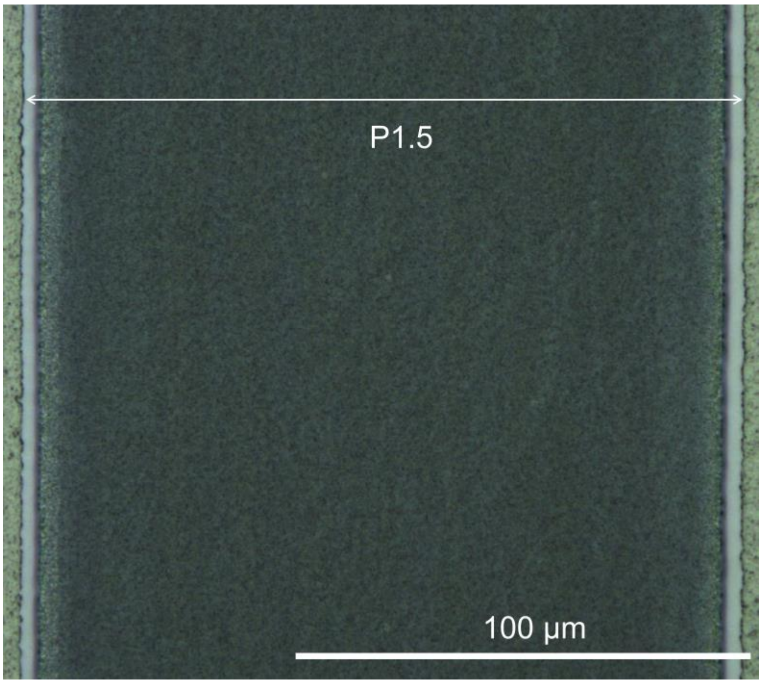


**Supplementary Fig. 12 |** Optical microscope image of P1.5.

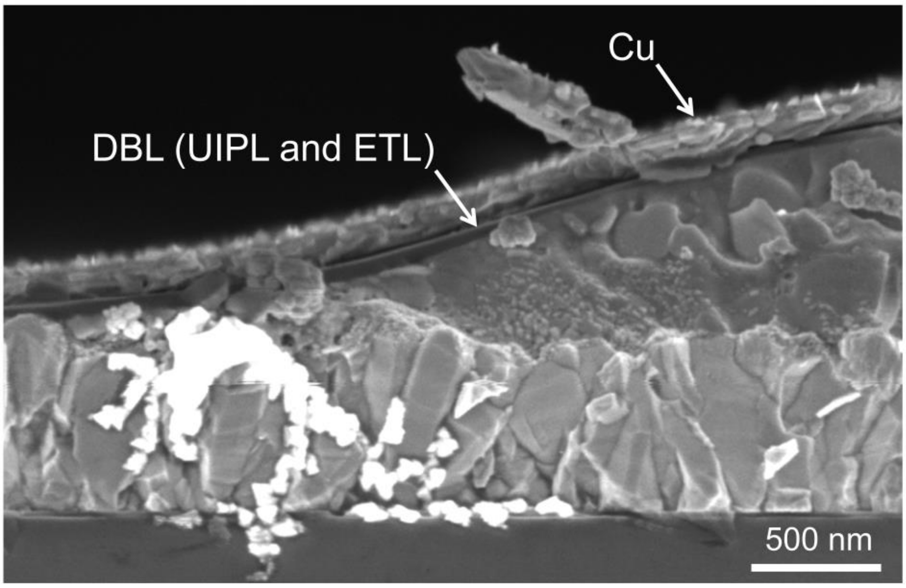


**Supplementary Fig. 13 |** Cross-sectional SEM image of the interconnected region of the module with P1.5 (DBL).

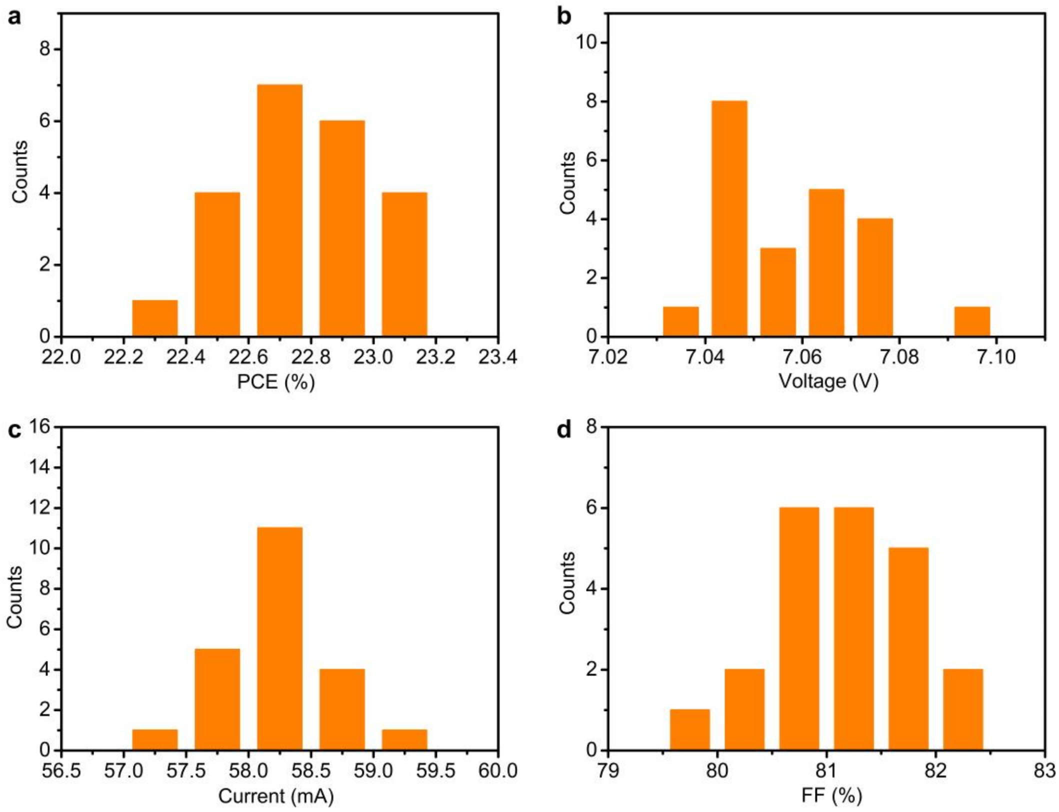


**Supplementary Fig. 14 |** Statistical distribution of (**a**) PCE, (**b**) $V_{OC}$, (**c**) $I_{SC}$ and (**d**) FF obtained from *I*-*V* curves of large-area (aperture area 14.625 $cm^2$) modules based on LTSG and P1.5. The average aperture area PCE of these modules is 22.79% and the highest is 23.2%.

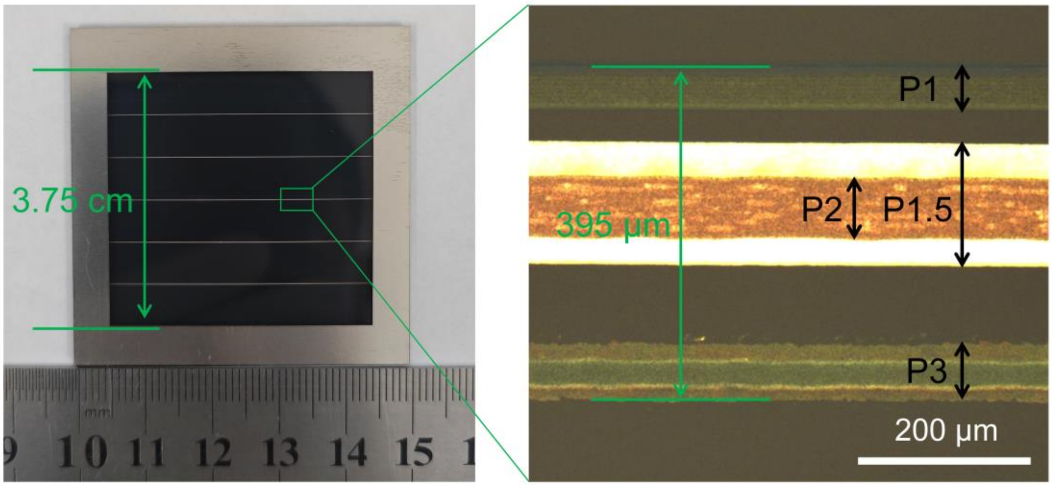


**Supplementary Fig. 15 |** Photo of module with metal masks. The geometric fill factor (GFF) calculation result is $GFF = (3.75\ cm - 5 \times 0.0395\ cm) \div 3.75\ cm = 94.7\%$.

| mks Newport | ACCREDITED Calibration Cert. # 2893.01 | Technology and Application Center **PV Lab** Newport Calibration Cert. # 2784 |
|---|---|---|

**DUT S/N:** 7311923-m5
**Newport Calibration #: 2784**
**Manufacturer:** Institute of Semiconductors, Chinese Academy of Sciences
**Material (single junction):** Perovskite
**Measurement Date:** 12-JUL-2023
**Temperature Sensor:** TC-K, DUT Temperature: 24.9 ± 0.8 °C
**Environmental conditions at the time of calibration:** Temperature: 24 ± 3 °C; Humidity: 30 ± 20 %

The above DUT has been tested using the following methods to meet the ISO 17025 Standard by the PV Lab at Newport Corporation. Quoted uncertainties are expanded using a coverage factor of $k = 2$ and expressed with an approximately 95% level of confidence. Measurement of total irradiance is traceable to the World Radiometric Reference (WRR) and all other measurements and uncertainties are traceable to NIST and the International System of Units (SI). The performance parameters reported in this certificate apply only at the time of the test, and do not imply future performance.

***Designated area as defined by thin metal aperture mask.**

**†Reported performance parameters were measured under a 10-point IV sweep configuration wherein the bias voltage (current for Voc determination) is held constant until the measured current (voltage for Voc) is determined to be unchanging at the 0.07% level. This is intended to represent the quasi-steady-state performance of the device. Total IV measurement time under these conditions was approximately 6 minutes.**

| | | | | | | | | | | | |
|---|---|---|---|---|---|---|---|---|---|---|---|
| Efficiency [%] | 22.73† | ± | 0.72 | V_oc [V] | 7.098 | ± | 0.054 | I_sc [A] | 0.0588 | ± | 0.0012 |
| P_max [mW] | 332.1 | ± | 9.8 | V_max [V] | 6.094 | ± | 0.087 | I_max [A] | 0.0545 | ± | 0.0012 |
| FF [%] | 79.5 | ± | 1.5 | Area [cm²] | 14.611* | ± | 0.031 | M | 0.985 | ± | 0.015 |

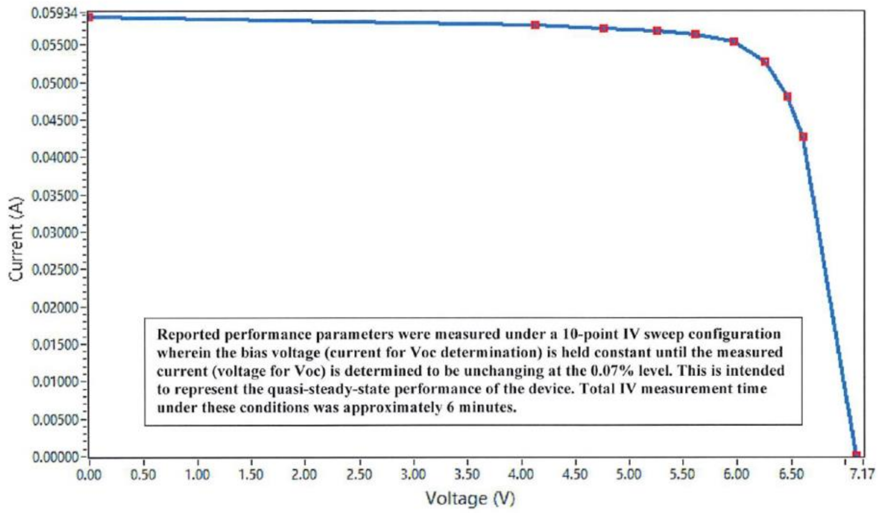


**Supplementary Fig. 16 |** Certificated results from an accredited photovoltaic certification laboratory (Newport, USA). The certificated efficiency is 22.73%. A mask with an aperture area was 14.611 cm$^2$ was used for the test. The $V_{OC}$ is 7.098 V, $I_{SC}$ is 58.8 mA, FF is 79.5%. The current-voltage performance parameters were measured under a 10-point IV sweep configuration wherein the bias voltage (current for $V_{OC}$ determination) is held constant until the measured current (voltage for $V_{OC}$) is determined to be unchanging at the 0.07% level. This is intended to represent the quasi-steady-state performance of the device. Total $I$-$V$ measurement time under these conditions was approximately 6 min.

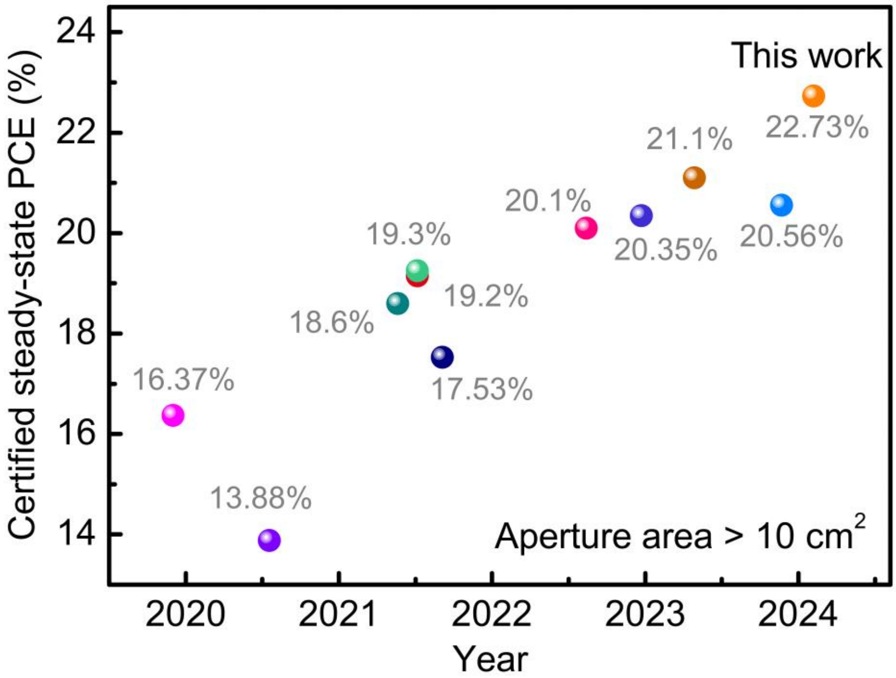


**Supplementary Fig. 17 |** Summary of reported perovskite solar mini-modules.

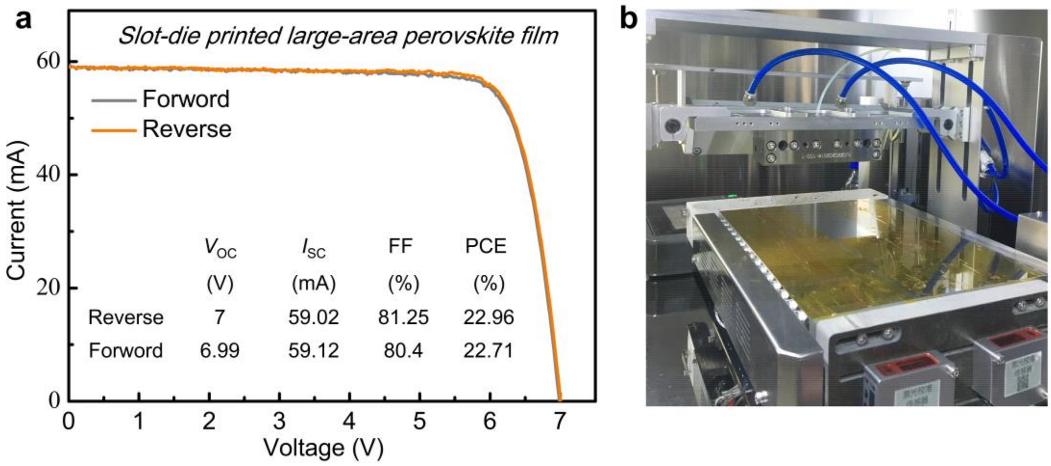


**Supplementary Fig. 18 | a,** *I-V* curves and performance parameters of large-area module (aperture area 14.625 $cm^2$) fabricated by slot-die printed perovskite precursor wet films, combined with our LTSG and P1.5 solutions. **b,** Slot-die system (purchased from Datamaker).

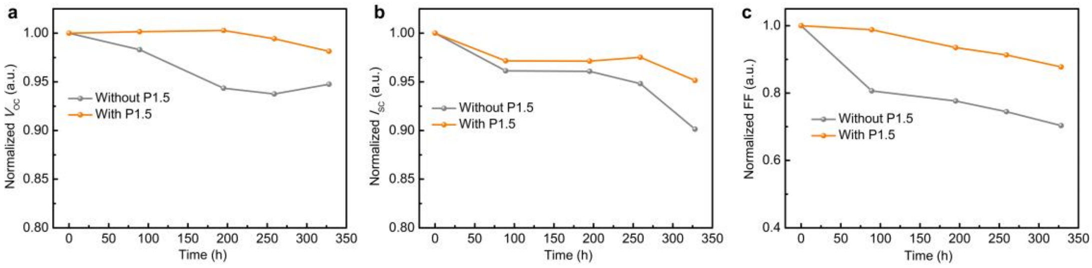


**Supplementary Fig. 19 |** Performances of perovskite modules in air aging experiments at 25 ºC and 30-40% relative humidity.

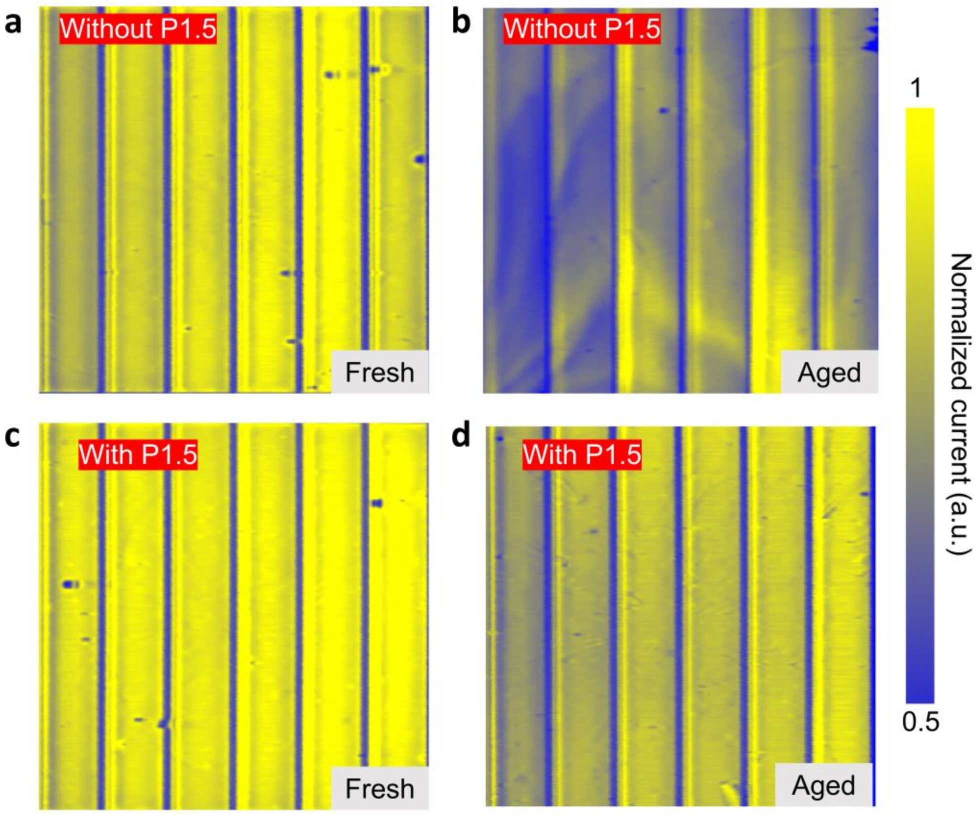


**Supplementary Fig. 20 |** Light (532 nm) beam induced current (LBIC) mapping images of perovskite solar modules with and without P1.5 (DBL) before and after air ambient aging.

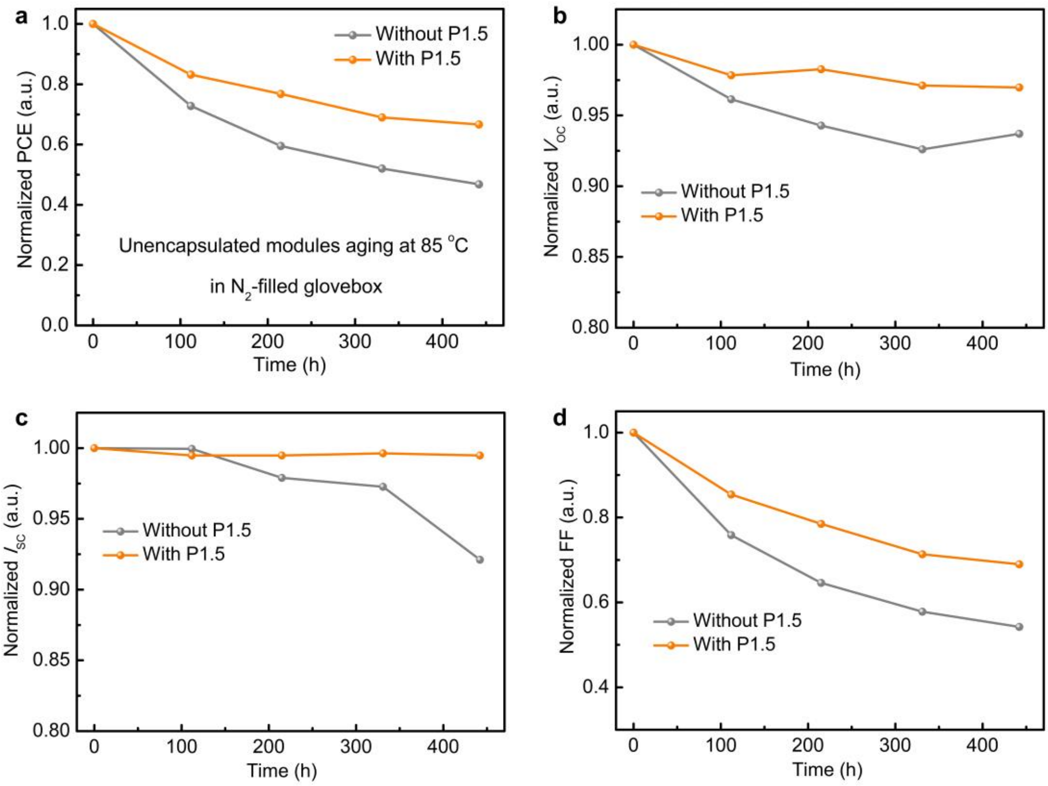


**Supplementary Fig. 21 |** Thermal stability tracking of the modules heated on an 85 °C hotplate in a $N_2$ glove box.

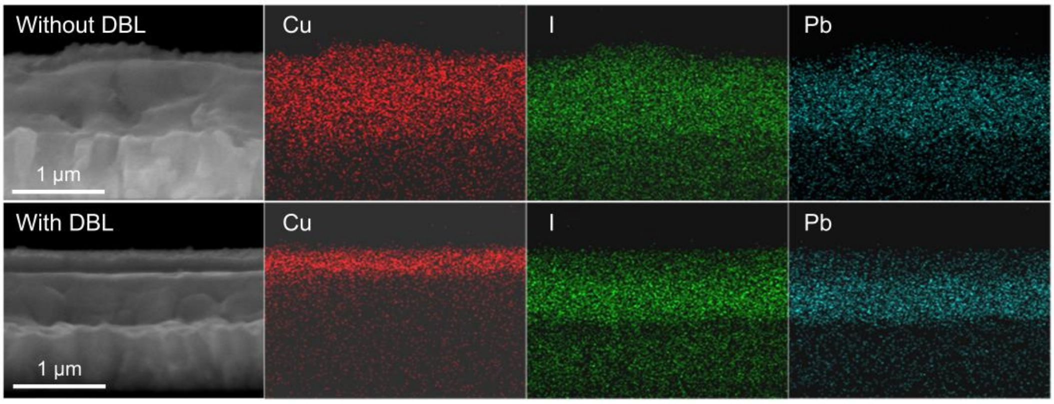


**Supplementary Fig. 22 |** SEM-EDX elemental distributions of glass/FTO/perovskite/Cu and glass/FTO/perovskite/PEACl/PCBM/$SnO_2$/Cu (similar to intercalation and non-intercalation of DBL at the interface of perovskite and Cu) after thermal aging at 85 ºC.

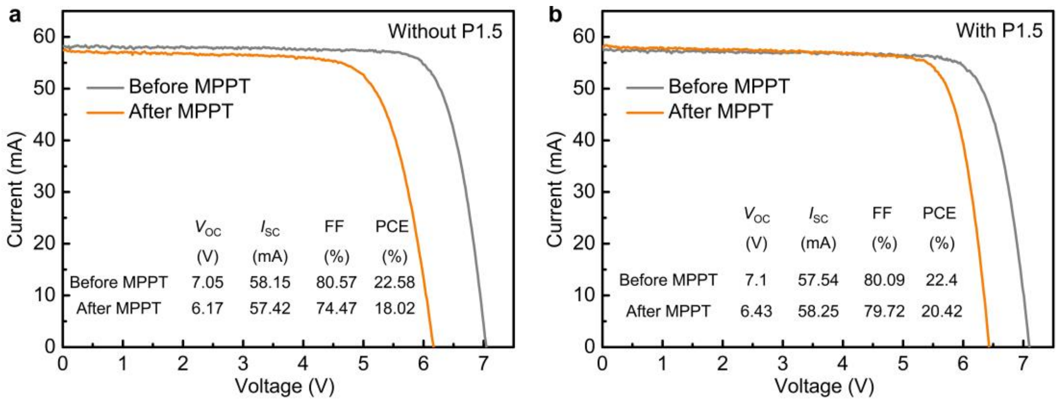


**Supplementary Fig. 23 |** *I-V* curves and performance parameters of perovskite modules before and after (a) 600 hours maximum power point tracking (MPPT), and (b) 1000 hours MPPT.

**Supplementary Table 1 |** Parameters of forward and reverse scan *I-V* curves of modules with and without P1.5 (DBL).

| | $V_{OC}$ (V) | $I_{SC}$ (mA) | FF (%) | PCE (%) |
|---|---|---|---|---|
| Without P1.5 (Forword) | 7.068 | 58.32 | 80.56 | 22.71 |
| Without P1.5 (Reverse) | 7.096 | 58.06 | 82.12 | 23.13 |
| With P1.5 (Forword) | 7.076 | 58.39 | 81.04 | 22.89 |
| With P1.5 (Reverse) | 7.092 | 58.28 | 81.83 | 23.13 |

**Supplementary Table 2 |** Structure, aperture area, and PCE of reported small-area and large-area devices.

| Device structure | Aperture area ($cm^2$) | Aperture area PCE (%) | Ref. |
|---|---|---|---|
| ITO/$SnO_2$/perovskite/spiro-OMeTAD/Ag or Au | 0.06 | 25 | *Nature* 620, 323-327 (2023) |
| | 27.83 | 21.4 | |
| ITO/$SnO_2$/perovskite/Organic HTL/Ag or Au | 1 | 23.5 | *Science* 379, 288-294 (2023) |
| | 17.1 | 21.4 | |
| ITO/PTAA/perovskite/$C_{60}$/BCP/Cu | 0.07 | 23.8 | *Science* 373, 902-907 (2021) |
| | 17.9 | 20.1 | |
| | 50.1 | 19.7 | |
| FTO/$TiO_2$/$SnO_2$/perovskite/spiro-MeOTAD/Au | 0.085 | 25.09 | *Nat. Sustainability* 6, 1465-1473 (2023) |
| | 12.25 | 20.75 | |
| FTO/$SnO_2$/perovskite/spiro-OMeTAD/Au | 0.16 | 24.02 | *Nat. Energy* 7, 528-536 (2022) |
| | 22.4 | 20.5 | |
| ITO/PTAA/perovskite/$C_{60}$/BCP/Cu | 0.08 | 24.6 | *Science* 380, 823-829 (2023) |
| | 26.9 | 21.8 | |
| ITO/PTAA/$Al_2O_3$/perovskite/$C_{60}$/$SnO_2$/Ag | 0.09 | 23.21 | *Adv. Mater.* 36, 2309310 (2024) |
| | 12.84 | 20.88 | |
| ITO/$SnO_2$/perovskite/spiro-OMeTAD/Au | 0.09 | 21.8 | *Nat. Energy* 5, 596-604 (2020) |
| | 22.4 | 16.6 | |
| ITO/$NiO_x$/PTAA/perovskite/PCBM/BCP/Ag | 0.05979 | 24.7 | *Energy Environ. Sci.* 16, 557-564 (2023) |
| | 19.3 | 21.6 | |
| ITO/PTAA/perovskite/$C_{60}$/BCP/metal | 0.08 | 21.3 | *Sci. Adv.* 5, eaax7537 (2019) |
| | 63.7 | 16.9 | |
| FTO/$TiO_2$/$SnO_2$/perovskite/spiro-MeOTAD/Au | 0.0803 | 25.7 | *Science* 375, 302-306 (2022) |
| | 1 | 23.3 | |
| | 20.92 | 20.75 | |
| | 66.95 | 19.7 | |
| FTO/$NiO_x$/Me-4PACz/perovskite/PCBM/$SnO_2$/Cu | 0.0737 | 24.93 | **This work** |
| | 14.625 | 23.2 | |

**Supplementary Table 3 |** Open circuit voltage, short circuit current density, fill factor and efficiency of small and large area champion efficiency devices.

| | $V_{OC}$ (V) | $J_{SC}$ (mA cm$^{-2}$) | FF (%) | PCE (%) |
|---|---|---|---|---|
| Small area device | 1.187 | 25.36 | 82.75 | 24.93 |
| Large area device | 7.073/6 = 1.179 | (58.47/14.625)*6 = 23.99 | 82.03 | 23.2 |

**Supplementary Table 4 |** Structure, certified steady-state PCE, and aperture area of the reported mini-modules.

| **Device structure** | **Aperture area ($cm^2$)** | **Certified steady-state PCE (%)** | **Ref.** |
|---|---|---|---|
| ITO/PTAA/perovskite/$C_{60}$/BCP/metal | 63.7 | 16.37 | *Sci. Adv.* 5, eaax7537 (2019) |
| ITO/$SnO_2$/perovskite/spiro-OMeTAD/Au | 22.26 | 13.88 | *Nat. Energy* 5, 596-604 (2020) |
| ITO/PTAA/perovskite/$C_{60}$/BCP/Cu | 30 | 18.6 | *Nat. Energy* 6, 633-641 (2021) |
| ITO/PTAA/perovskite/$C_{60}$/BCP/Cu | 18.1 | 19.3 | *Science* 373, 902-907 (2021) |
| | 50 | 19.2 | |
| FTO/$TiO_2$/perovskite/Spiro/Au | 31 | 17.53 | *Joule* 5, 2420-2436 (2021) |
| ITO/PTAA/$Al_2O_3$/perovskite/$C_{60}$/$SnO_2$/Ag | 12.84 | 20.1 | *Adv. Energy Mater.* 12, 2202287 (2022) |
| ITO/$NiO_x$/PTAA/perovskite/PCBM/BCP/Ag | 18.52 | 20.35 | *Energy Environ. Sci.* 16, 557-564 (2023) |
| ITO/PTAA/perovskite/$C_{60}$/BCP/Cu | 26.9 | 21.1 | *Science* 380, 823-829 (2023) |
| ITO/PTAA/$Al_2O_3$/perovskite/$C_{60}$/$SnO_2$/Ag | 12.84 | 20.56 | *Adv. Mater.* 36, 2309310 (2024) |
| FTO/$NiO_x$/Me-4PACz/perovskite/PCBM/$SnO_2$/Cu | 14.61 | 22.73 | **This work** |